SCIENCE CHINA
Technological Sciences

•Article•

June 2024 Vol.67 No.6: 1685–1694
https://doi.org/10.1007/s11431-023-2481-4

Numerical study on the effective thermal conductivity and thermal tortuosity of porous media with different morphologies

DU Shen, LI Dong, LI Meng-Jie & HE Ya-Ling*

Key Laboratory of Thermo-Fluid Science and Engineering of Ministry of Education, School of Energy and Power Engineering, Xi'an Jiaotong University, Xi'an 710049, China

Received May 19, 2023; accepted August 3, 2023; published online May 21, 2024

Effective thermal conductivity and thermal tortuosity are crucial parameters for evaluating the effectiveness of heat conduction within porous media. The direct pore-scale numerical simulation method is applied to investigate the heat conduction processes inside porous structures with different morphologies. The thermal conduction performances of idealized porous structures are directly compared with real foams across a wide range of porosity. Real foam structures are reconstructed using X-ray computed tomography and image processing techniques, while Kelvin and Weaire-Phelan structures are generated through periodic unit cell reconstruction. The detailed temperature fields inside the porous structures are determined by solving the heat conduction equation at the pore scale. The results present that the equivalent thermal conductivity of Kelvin and Weaire-Phelan structures is similar to and greater than that of the real foam structure with the same strut porosity. The thermal tortuosity of real foam structure is relatively larger and the heat conduction path becomes straighter by adopting the anisotropic design. The thermal tortuosity of the fluid channels for Kelvin, Weaire-Phelan, and real foam structures is close to one. The thermal conductivity of porous structures with heat transfer fluid increases as the thermal conductivity ratio of fluid to solid becomes larger. A small porosity of porous media leads to a larger equivalent thermal conductivity due to the dominant contribution of porous skeleton in the heat conduction process. Correlations derived from parallel and series models, as well as the Maxwell-Eucken models, provide decent predictions of effective thermal conductivity, with an average error of less than 8% in the entire range of thermal conductivity ratio.

volumetric solar receiver, porous morphology, direct pore-scale simulation, equivalent thermal conductivity, thermal tortuosity, empirical correlation

Citation: Du S, Li D, Li M J, et al. Numerical study on the effective thermal conductivity and thermal tortuosity of porous media with different morphologies. Sci China Tech Sci, 2024, 67: 1685–1694, https://doi.org/10.1007/s11431-023-2481-4

1 Introduction

Reticulated porous media possess distinct features, such as a large specific surface area, interconnected flow channels, high effective thermal conductivity, and lightweight, making them widely applicable in various energy-related fields. Researchers have extensively investigated metallic and ceramic porous foams as heat exchangers, combustion chambers, volumetric solar receivers, and thermally conductive skeletons in thermal energy storage systems [1–5]. Determining transport properties such as permeability, effective thermal conductivity, convective heat transfer coefficient, and extinction coefficient of the porous media is crucial to enhancing performance [6,7]. Among different energy-related applications, thermal conductivity is a fundamental parameter to evaluate heat conduction efficiency. For example, the thermal conductivity of a porous skeleton significantly influences the temperature field and local heat spot of a volumetric solar receiver. Therefore, accurately determining thermal conductivity is necessary, and quanti-

*Corresponding author (email: yalinghe@mail.xjtu.edu.cn)

tatively evaluating the heat conduction path inside the porous media is essential. Despite the experimental measurement, the direct pore-scale numerical method is an effective tool for studying the heat conduction process inside complex three-dimensional (3D) structures.

Computed tomography (CT) scan with different resolutions (30 and 1 μm) was applied by Petrasch et al. [8] to investigate the effective thermal conductivities of porous ceramics at macroscopic and microscopic levels. At the macroscopic level, the influences of porosity and ratio of fluid and strut thermal conductivities on the effective thermal conductivities were analyzed. At the microscopic level, the influence of the ratio of the fluid-to-solid thermal conductivities was investigated. Reliable correlations were found to predict the thermal conductivity of both macroscopic porous foams and microscopic porous struts. Zafari et al. [9] measured the non-isotropic effective thermal conductivities of aluminum and copper foams with different porosities by direct pore-scale simulation. This study highlighted the significant impact of the thermal conductivity of a solid on the overall thermal conductivity of the porous foam. Ranut et al. [10] performed direct pore-scale simulation on the μ-CT-based reconstructed aluminum metal foams with different pore densities. Under similar porosity, the metal foam with a smaller pore size exhibited larger effective thermal conductivity. However, in the study of Bodla et al. [11], the effective thermal conductivity did not monotonically change with pore density under similar porosities. Ranut et al. [12] also measured the effective thermal conductivity of aluminum metal foams with different pore densities containing air and water. The anisotropy of effective thermal conductivity was apparent in the porous foam with smaller pore sizes, where heat was efficiently conducted along the direction of elongation of the pore cells. Moreover, the thermal conductivity of fluids did not significantly influence the overall effective thermal conductivity due to the large difference in thermal conductivities between fluid and solid.

In addition, due to the complex nature of the real porous foams and the redundant procedure of the X-ray CT reconstruction, idealized structures such as cubic, Kelvin, and Weaire-Phelan structures are often used to represent porous foams in simulations. Mendes et al. [13] evaluated the effective thermal conductivities of the cubic cell and Kelvin cell with different porosity and lump structures. The effective thermal conductivity of cubic and Kelvin cells was close when the dimensions of strut and lump were identical. A simplified model based on the various bounds of thermal conductivities such as serial/parallel bounds, Hashin-Shtrikman bounds, and effective medium theory bound is proposed, of which the applicability was tested with real open-cell foam structures generated by 3D CT scan. Bianchi et al. [14] and Bracconi et al. [15] investigated the effective thermal conductivity of periodic open cellular porous structures (cubic cell and tetrakaidecahedral cell) and Voronoi-tessellation-based porous foam, respectively, with different ratios between node and strut diameters. It was found that reducing the strut cross-sectional area deteriorated the heat conduction performance. Fiedler et al. [16] compared the effective thermal conductivities of real and idealized cellular aluminum structures using the lattice Monte Carlo approach and transient plane source method. The thermal conductivity of real M-pore porous foam was slightly higher than that of the inverted face-centered cubic and open-cell model structures under the same porosity. Based on the lattice Boltzmann method, the effective thermal conductivity of lattice structures with different topologies was studied by Wang et al. [17]. An averaged correlation of effective thermal conductivity for the cube, FD-cube, tetrakaidecahedron, and octet structures in the entire range of porosity was proposed.

On the other hand, tortuosity is a significant factor in measuring the impact of porous structure on various transport processes, including fluid flow, molecular diffusion, electrical conduction, and heat conduction [18]. However, there is no consistent definition of tortuosity, and both geometrical and physical tortuosities are widely used. When considering the heat conduction in porous media, thermal tortuosity should be applied, as it is closely related to effective thermal conductivity. Thermal tortuosity is used to evaluate the tortuous path of heat conduction in porous structures. Larger thermal tortuosity signifies an inefficient heat conduction channel inside the porous domain. Bodla et al. [11] calculated the geometrical tortuosity of a porous skeleton with different pore densities in three directions by the nodal network using commercial software Amira. The geometrical tortuosity ranged from 2.15 to 3.31, and no anisotropy was seen due to the limitation of sample size. Haussener et al. [19] performed the pore-scale simulation for the reticulate porous ceramic and determined its effective thermal conductivity and tortuosity. The tortuosity in this study was defined based on the velocity distribution and had a mean value of 1.07. Kumar et al. [20] determined the fluid tortuosity and skeleton tortuosity respectively for different porous structures. The fluid tortuosity was close to one, while the skeleton tortuosity ranged from 1 to 1.2. The geometrical tortuosity of spherical and polyhedral porous networks was studied by Xu et al. [21] based on the continuum percolation theory. The influence of porosity near the percolation threshold and above as well as the pore shape was analyzed.

Based on the above analyses, it is apparent that the thermal tortuosity of porous foams has often been overlooked when investigating heat conduction within these structures. Instead, geometrical tortuosity is typically used as a substitute for thermal tortuosity. One advantage of porous foam that offers tortuous channels is questionable and the heat conduction path inside different porous structures should be quantitively determined. Moreover, the impact of the mor-

phology and complexity of the geometrical structures on the effective thermal conductivity and thermal tortuosity of porous foams has not been fully explored. Randomly and periodically distributed porous skeletons exhibit varying heat conduction properties, resulting in differences in heat conduction performance. Therefore, a comprehensive comparison of heat conduction processes between real foam structures and idealized periodic unit cells across a wide range of porosity is necessary. The reconstruction procedures of Kelvin, Weaire-Phelan, and real foam structures are elaborated in Section 2. The direct pore-scale numerical simulation method to determine the heat conduction process inside the porous structures is presented in Section 3. The effective thermal conductivity of the porous skeleton, fluid channel, and combination of these two zones is analyzed and the thermal tortuosity of the porous skeleton and fluid channel is determined in Section 4.

2 Porous structures reconstruction

Pore-scale numerical simulation relies on porous media reconstruction. With advancements in X-ray imaging techniques, the real foam structure can be captured via X-ray computed tomography [22]. The real porous sample is scanned by the YXLON Cheetah X-ray inspection system in this study. The rendered cross-sectional images provide the 3D geometry of the porous structure. The quality of the geometry and unstructured grid could be further improved by diagnosing and repairing the structures. The detailed reconstruction method could refer to the previous publication [23]. Moreover, the geometrical parameters of the porous structure could be adjusted according to reference [24] and the influence of porosity on the heat transfer process could be analyzed. The representative volume of the real foam is presented in Figure 1(a).

On the other hand, simplified unit structure reconstruction methods are widely used to avoid the complexity of X-ray computed tomography reconstruction. Kelvin and Weaire-Phelan structures are commonly used to represent idealized foams with equal-sized bubbles. The Kelvin structure has six quadrilateral and eight hexagonal faces, whereas the Weaire-Phelan structure consists of an irregular dodecahedron and a truncated hexagonal trapezohedron. To generate the Kelvin and Weaire-Phelan structures, the software Surface Evolver is applied in this study. The vertices coordinate and their connections are captured which are imported to the CAD software for the porous frame reconstruction. For simplicity, the porous skeleton has a cylindrical shape and the porosity is adjusted by changing the strut diameter. The unit cells of Kelvin and Weaire-Phelan structures are presented in Figure 1(b) and (c), respectively.

Based on the reconstruction method described above, real foam, Kelvin, and Weaire-Phelan structures with various porosities are generated and summarized in Table 1. The strut thickness of all structures is adjusted in order to guarantee the porosity is roughly in the range of 0.75–0.90.

3 Numerical modeling

3.1 Direct pore-scale numerical simulation

The acquisition of detailed temperature fields is necessary to analyze the effective thermal conductivity and thermal

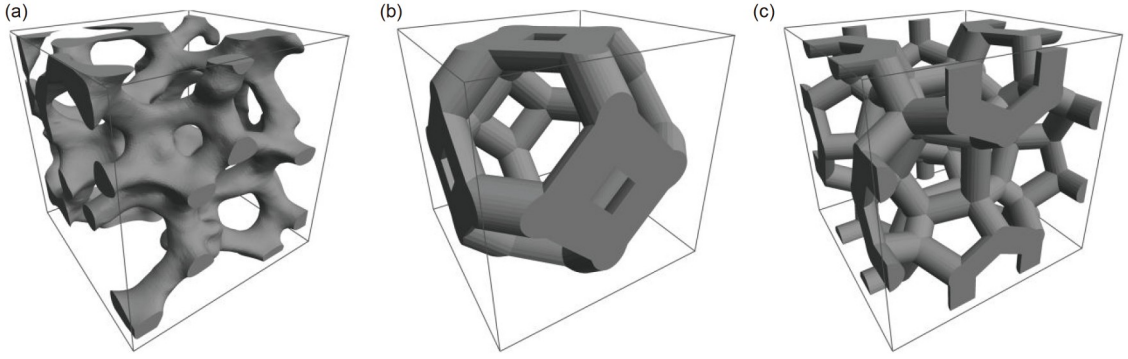

Figure 1 Representative volume of real foam (a), Kelvin structure (b), and Weaire-Phelan structure (c).

Table 1 Porosity of different porous structures

Samples	Porosity	Dimension
Real foam A, B, C, D	0.734, 0.789, 0.838, 0.886	6 mm×7 mm×19 mm
Kelvin structures A, B, C, D	0.750, 0.795, 0.837, 0.876	1 mm×1 mm×5 mm
Weaire-Phelan structures A, B, C, D	0.757, 0.794, 0.861, 0.891	2 mm×2 mm×13 mm

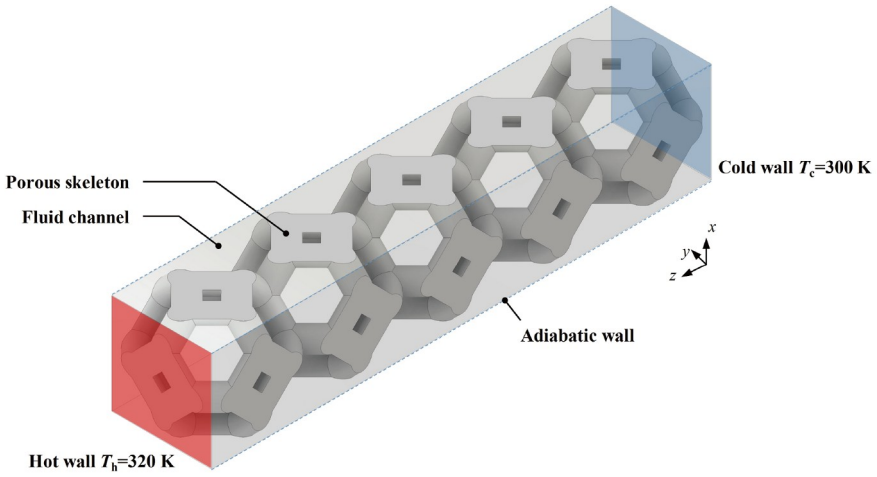

Figure 2 (Color online) Illustration of boundary conditions for thermal conductivity calculation.

tortuosity of porous structures. For this purpose, the steady-state heat conduction equation as presented in eq. (1) is solved for real foam, Kelvin, and Weaire-Phelan structures. In the equation, λ is the thermal conductivity of the bulk material.

$$\frac{\partial}{\partial x_j}\left(\lambda\frac{\partial T}{\partial x_j}\right)=0. \tag{1}$$

Taking Kelvin structure as an example, the boundary conditions are illustrated in Figure 2. The entire domain is divided into two parts which are a porous skeleton and a fluid channel. The outer surface of the porous skeleton represents the interface between these two parts. The solid walls at the inlet and outlet are maintained at a constant temperature of 320 and 300 K, respectively. When considering the heat transfer inside the porous skeleton, the fluid channel zone is deleted and the porous surface is set as an adiabatic wall. A similar treatment is applied when considering the heat transfer inside the fluid channel. When the thermal conductivity of both porous skeleton and fluid channel is investigated, the heat conduction in the two zones is solved and the interface is set as a coupled wall boundary condition. In all simulation cases, the four lateral walls are considered adiabatic.

The unstructured meshes are generated for different porous structures within the commercial software ANSYS ICEM. Meshes with different numbers of elements are generated and the simulation results are compared in order to check mesh independence. The Finite Volume Method is applied for discretizing the heat conduction equation, which is solved with the commercial software ANSYS Fluent. The temperature field is considered to be converged as the absolute value of residual reaches 1×10^{-6}. The bulk thermal conductivity of the bulk material is assumed to be constant.

3.2 Numerical model validation

First, mesh-independent results are checked for simulations in Kelvin, Weaire-Phelan, and foam structures. For instance, the node number exceeding 2.5×10^5 is selected for Kelvin structures in the heat conduction simulations. To assess the accuracy of the current numerical model, the results of pore-scale numerical simulations are compared with experimental findings from reference [25]. The simulation conditions are set to match those of the experiment. The fluid and solid phases consist of air and alumina, respectively. The thermal conductivity of alumina is estimated based on the porosity and thermal conductivity of the struts. The comparison is illustrated in Figure 3, demonstrating an agreement between numerical and experimental results. The largest discrepancy occurs when the porosity is higher, reaching a maximum error of 12%.

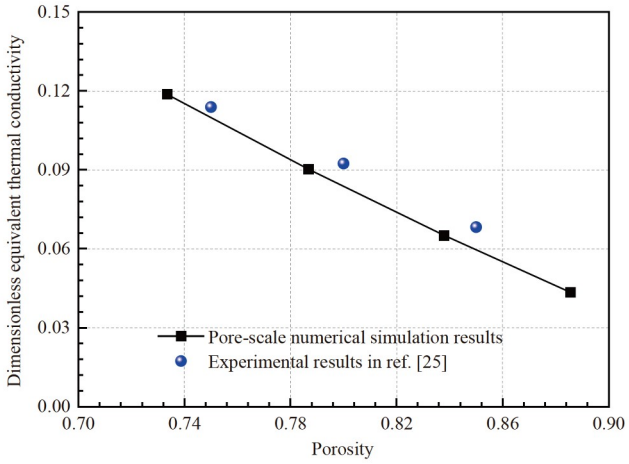

Figure 3 (Color online) Comparison of the simulation results with the experimental data.

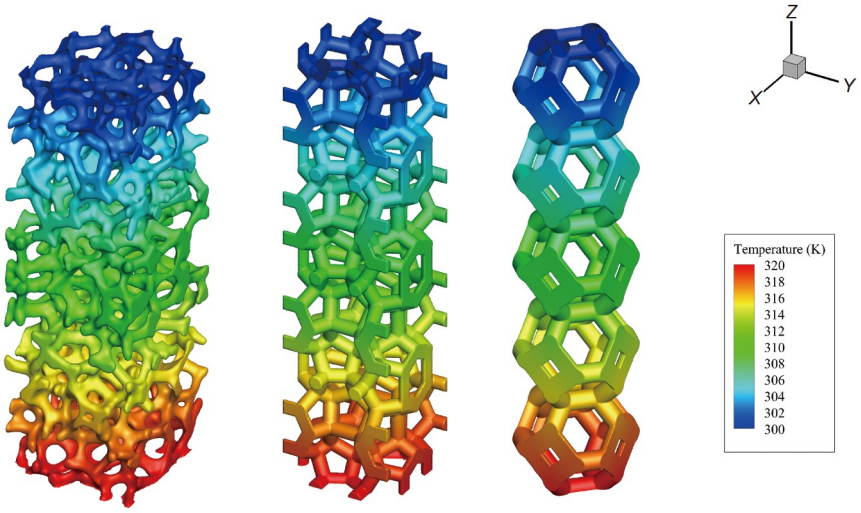

Figure 4 Temperature fields inside different porous structures.

4 Results and discussion

4.1 Influence of porosity on the effective thermal conductivity and thermal tortuosity

The temperature fields of various porous structures under constant temperature boundary conditions are presented in Figure 4. Due to the direct pore-scale simulation method, the detailed heat transfer processes inside the porous skeletons could be visualized.

Temperature distribution within the porous structure primarily follows a one-dimensional assumption, with the main variation occurring along the z-axis. However, local temperature non-uniformity is noticed in the real porous foam due to the stochastic nature of the skeleton. Moreover, Kelvin and Weaire-Phelan structures exhibit periodic temperature fluctuation resulting from the periodic arrangement of single unit cell, which is demonstrated by the average temperature distribution as presented in Figure 5.

Figure 6 presents the equivalent thermal conductivity λ_{eff} and the thermal tortuosity τ_{t} of different porous structures based on eqs. (2) and (3), respectively. In these equations, q is the heat flux, ε_{p} represents the fraction of the volume of the porous skeleton to the total volume of space, and λ_0 is the bulk thermal conductivity. The thermal tortuosity is related to the ratio of bulk and effective thermal conductivity, which could be further expressed by heat flux transferring through the porous domain and the bulk domain with the same dimensions based on Fourier's law. The dimensionless equivalent thermal conductivity is defined as the ratio of equivalent thermal conductivity to the bulk thermal conductivity of the material. It is worth noting that ε_{p} does not equal the porosity ε normally defined in porous foam. When considering the heat conduction in a porous skeleton, the strut porosity ε_{p} should be used.

$$\lambda_{\text{eff}} = q_{\text{eff}} / \frac{\mathrm{d}T}{\mathrm{d}x}, \tag{2}$$

$$\tau_{\text{t}} = \sqrt{\varepsilon_{\text{p}} \cdot \frac{\lambda_0}{\lambda_{\text{eff}}}} = \sqrt{\varepsilon_{\text{p}} \cdot \frac{q_0}{q_{\text{eff}}}}. \tag{3}$$

In Figure 6(a), the thermal conductivity of the porous skeleton increases with increasing strut porosity, owning to the thicker porous skeleton that is beneficial for heat conduction. In comparison, the thermal conductivity of porous foam is relatively lower than those of Kelvin and Weaire-Phelan structures for the same strut porosity. The thermal tortuosity of the different structures, calculated as shown in Figure 6(b), reveals that the porous foam is more tortuous than the other structures, which depends on the intrinsic geometry of the foam. Moreover, the similarity in the geometries of the Kelvin and Weaire-Phelan structures is verified due to their close equivalent thermal conductivity and thermal tortuosity, which is consistent with previous studies

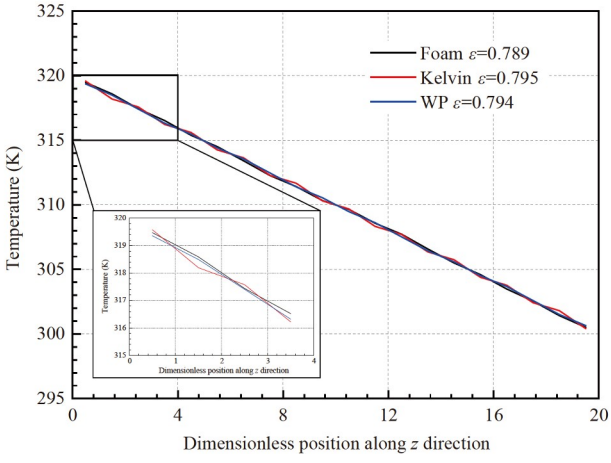

Figure 5 Average temperature distribution along z direction.

[26,27]. Furthermore, compared with other types of porous media with low porosity such as sandstone, the thermal tortuosity of the foam-type porous structures is relatively lower. It was reported in reference [18] that the thermal tortuosity of the Fontainebleau sandstone sample with a porosity of about 0.1 reached 3.5.

4.2 Influence of pore shape on the thermal tortuosity

Foam-type porous structures are typically assumed to have a spherical pore shape. Changing the pore shape breaks the homogeneity of heat conduction and requires reevaluating the thermal tortuosity of the porous media. The real foam, Kelvin and Weaire-Phelan structures are artificially scaled non-uniformly. The inset in Figure 7 shows the original Kelvin unit cell along with scaled Kelvin unit cells with scale factors of 1.5 and 2.0. Figure 7 summarizes the thermal tortuosity of porous structures with varying non-uniform scale factors.

The results demonstrate that the thermal tortuosity decreases in the scaled direction of the porous structures. For instance, in the case of the Kelvin structure, the thermal tortuosity decreases by a relative value of 10.4% and 15.4%, respectively, when the original Kelvin unit cell is scaled in the z direction by 1.5 and 2.0. Qualitatively, the thermal tortuosity measures the elongation of heat conduction paths, and the strut becomes straighter in the scaled direction. As a result, designing anisotropy can be used to optimize heat conduction within porous materials. Moreover, the real foam exhibits higher thermal tortuosity than Kelvin and Weaire-Phelan structures under different scale factors.

4.3 Thermal tortuosity of the fluid zone in the porous structures

The heat conduction inside the void zone of porous structures is mainly attributed to energy transfer in the heat transfer fluid. The equivalent thermal conductivity and thermal tortuosity of the fluid zone in porous structures are calculated and plotted in Figure 8. Firstly, an increase in channel

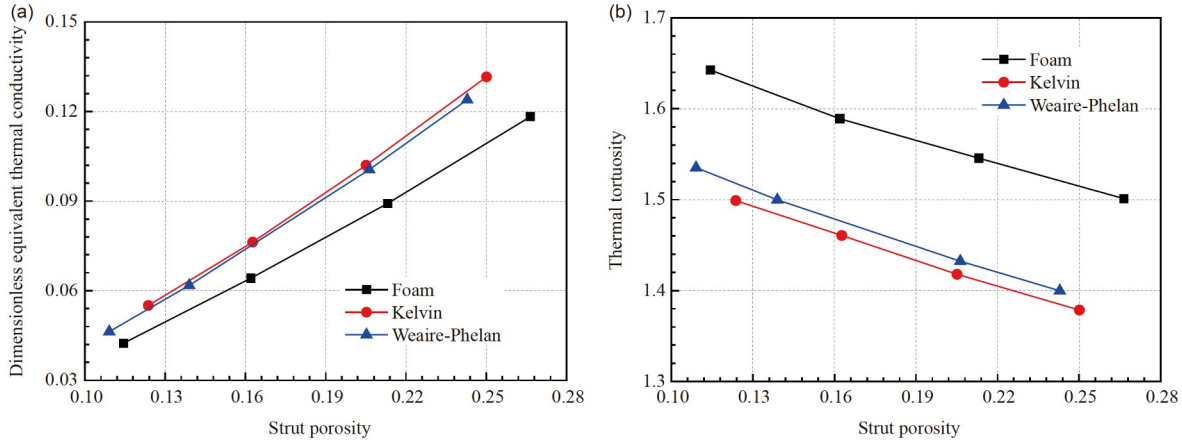

Figure 6 (Color online) (a) Dimensionless equivalent thermal conductivity; (b) thermal tortuosity of porous skeletons in different porous structures.

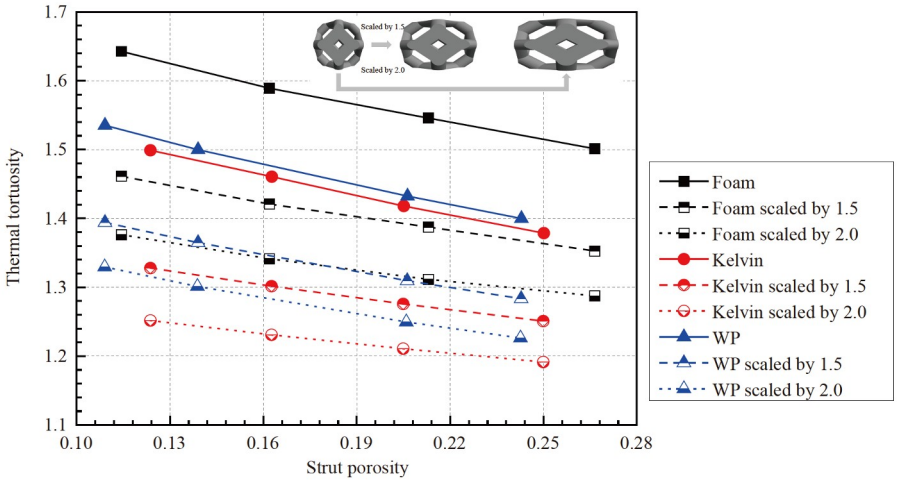

Figure 7 (Color online) Thermal tortuosity of porous structures with different non-uniform scale factors.

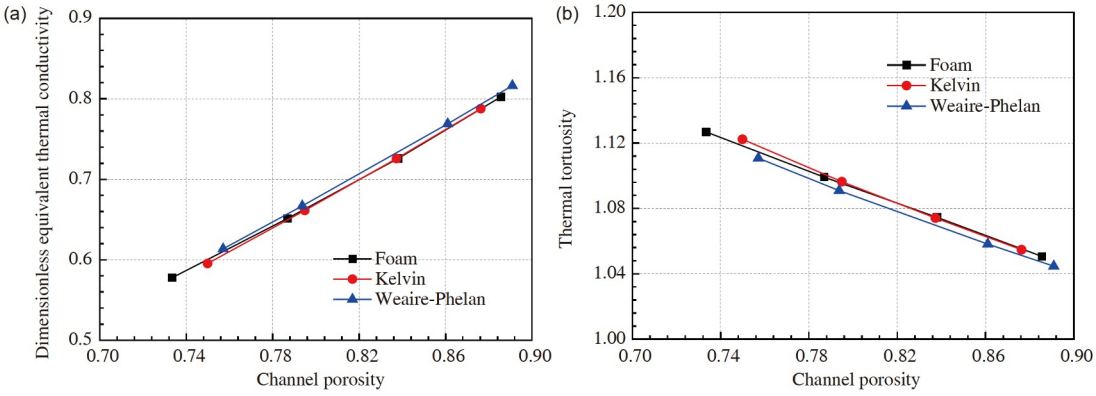

Figure 8 (a) Dimensionless equivalent thermal conductivity; (b) thermal tortuosity of fluid channels in different porous structures.

porosity results in an increase in the equivalent thermal conductivity and a decrease in thermal tortuosity. As the channel porosity increases, the fluid region in the porous structures increases, enabling more heat transfer fluid to participate in the heat conduction process. Secondly, no significant differences in the equivalent thermal conductivity and thermal tortuosity are observed among real foam, Kelvin and Weaire-Phelan structures. When compared with real foam structures, the maximum differences in equivalent thermal conductivity under the same porosity for Kelvin and Weaire-Phelan structures are 0.96% and 1.06%, respectively. Thirdly, the thermal tortuosity of the fluid zone in foam-type porous structures is relatively small and close to one. Prior studies have indicated that the tortuosity effect in foam-type porous structures with high porosity may sometimes be ignored [19,20,28].

4.4 Thermal conductivity of porous structures with different heat transfer fluids

Regarding an effective heat exchanger, the heat conduction in porous structures together with the heat transfer fluid should be analyzed. The equivalent thermal conductivity of porous structures with different heat transfer fluids is calculated and presented in Figure 9 in terms of the ratio of thermal conductivity between fluid and solid. If gas is considered as the heat transfer fluid within the metal foam, the thermal conductivity ratio of fluid and solid could reach 10^{-4}. Therefore, the range of thermal conductivity ratio is set to 10^{-4}–1.

Firstly, it is noticed from Figure 9 that the equivalent thermal conductivity of the fluid and solid increases as the thermal conductivity ratio becomes larger. This trend becomes apparent when the thermal conductivity ratio is greater than 0.1. When the thermal conductivity ratio equals one, the dimensionless equivalent thermal conductivity of the fluid and solid equals one. Compared with Figure 6(a), the equivalent thermal conductivity of the fluid and solid is close to that of the porous skeleton because heat conduction in the heat transfer fluid is negligible. Secondly, the equivalent thermal conductivity is larger in the entire range for the porous structure with small porosity due to the dominant contribution of the porous skeleton in the heat conduction process. However, the difference in the equivalent thermal conductivity becomes smaller as the thermal conductivity ratio gets larger.

To provide a rapid estimation of the thermal conductivity of porous media, several asymptotic models have been established [29]. The most commonly adopted models are the parallel and series models based on the mixing law, as shown in eqs. (4) and (5), respectively. These two models give a rough estimation for the highest and lowest values of the equivalent thermal conductivity. Additionally, the Maxwell-Eucken models provide narrow bounds for the equivalent thermal conductivity. The upper and lower bounds are presented in eqs. (6) and (7), respectively. Therefore, the thermal conductivity correlation could be generated as an arithmetic mean based on these bounds, as shown in eq. (8), where a and b are the constant to be determined by curve

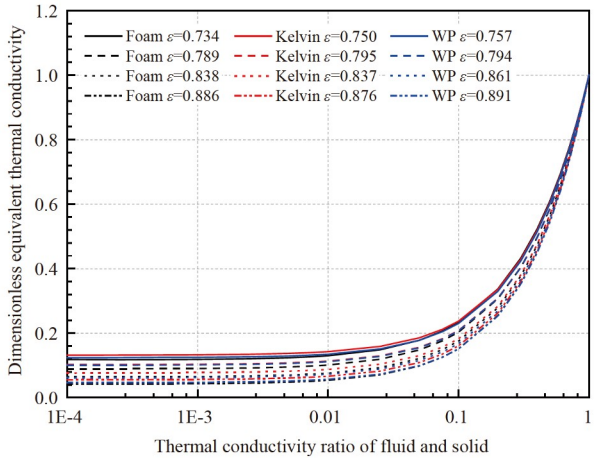

Figure 9 Dimensionless equivalent thermal conductivity of porous structures with different heat transfer fluids.

fitting. The comparison of different correlations based on thermal conductivity bounds, effective medium theory, and pore-scale simulation results are summarized in Figure 10.

$$\lambda_{//} = \lambda_{\mathrm{f}} \cdot \varepsilon + \lambda_{\mathrm{s}} \cdot (1-\varepsilon), \tag{4}$$

$$\lambda_{\perp} = [\varepsilon / \lambda_{\mathrm{f}} + (1-\varepsilon) / \lambda_{\mathrm{s}}]^{-1}, \tag{5}$$

$$\lambda_{\mathrm{ME,\,upper}} = \lambda_{s} \frac{2\lambda_{\mathrm{s}} + \lambda_{\mathrm{f}} - 2(\lambda_{\mathrm{s}} - \lambda_{\mathrm{f}}) \cdot \varepsilon}{2\lambda_{\mathrm{s}} + \lambda_{\mathrm{f}} + (\lambda_{\mathrm{s}} - \lambda_{\mathrm{f}}) \cdot \varepsilon}, \tag{6}$$

$$\lambda_{\mathrm{ME,\,lower}} = \lambda_{\mathrm{f}} \frac{3\lambda_{\mathrm{s}} - 2(\lambda_{\mathrm{s}} - \lambda_{\mathrm{f}}) \cdot \varepsilon}{3\lambda_{\mathrm{f}} + (\lambda_{\mathrm{s}} - \lambda_{\mathrm{f}}) \cdot \varepsilon}, \tag{7}$$

$$\begin{aligned} \lambda_{\mathrm{eff}} &= a \cdot \lambda_{//} + (1-a) \cdot \lambda_{\perp} \\ &= b \cdot \lambda_{\mathrm{ME,\,upper}} + (1-b) \cdot \lambda_{\mathrm{ME,\,lower}}, \end{aligned} \tag{8}$$

$$\begin{aligned} \lambda_{\mathrm{eff}} = \frac{1}{4}\Big[&\lambda_{\mathrm{f}} \cdot (3\varepsilon - 1) + \lambda_{\mathrm{s}} \cdot [3(1-\varepsilon) - 1] \\ &+ \sqrt{[\lambda_{\mathrm{f}} \cdot (3\varepsilon - 1) + \lambda_{\mathrm{s}} \cdot [3(1-\varepsilon) - 1]]^2 + 8 \cdot \lambda_{\mathrm{f}} \cdot \lambda_{\mathrm{s}}}\Big]. \end{aligned} \tag{9}$$

Figure 10 shows that the predictions of effective thermal conductivity by different models deviate from the pore-scale simulation results at low thermal conductivity ratios of fluid and solid. Compared with parallel and series models, the Maxwell-Eucken models provide the narrower bounds but the difference in lower bounds is not distinct as the thermal conductivity ratio of fluid and solid becomes smaller. The effective medium theory underestimates the effective thermal conductivity when the thermal conductivity ratio of fluid and solid is small and an accurate prediction could be obtained when the ratio exceeds 0.1. Moreover, the empirical correlations based on series and parallel models and Maxwell-Eucken models as presented in eq. (8) match well with

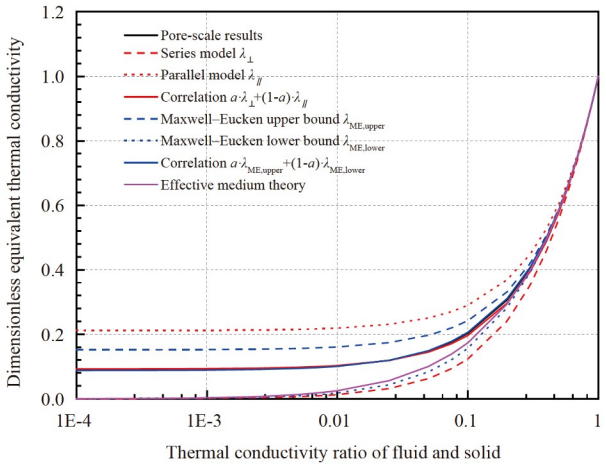

Figure 10 Dimensionless equivalent thermal conductivity based on pore-scale simulation and asymptotic models.

the pore-scale simulation results. Curve fitting determines the constants a and b, resulting in an R-square value greater than 0.99. The maximum and average errors predicted by these two empirical correlations are summarized in Figure 11.

In general, the two empirical correlations provide reliable predictions for the effective thermal conductivity over the entire range of thermal conductivity ratio of fluid and solid, with an average error lower than 8%. The correlation based on series and parallel models exhibits the highest error for porous structures with large porosity and low thermal conductivity ratios. Conversely, the narrow bounds provided by the Maxwell-Eucken models result in a relatively small maximum error, with the largest value below 10%. Therefore, the correlations shown in eq. (10) could be applied for the rapid estimation of equivalent thermal conductivity in various porous structures.

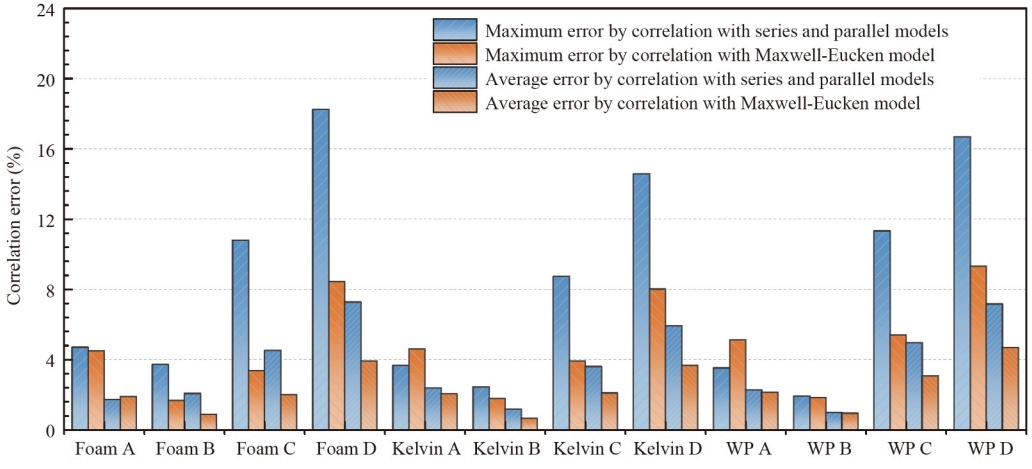

Figure 11 Maximum and average errors for the effective thermal conductivity correlations.

$$\lambda_{\text{eff}}=\begin{cases}0.4374\cdot\lambda_{//}+0.5626\cdot\lambda_{\perp}=0.5785\cdot\lambda_{\text{ME, upper}}+0.4215\cdot\lambda_{\text{ME, lower}} & \text{(Foam)},\\ 0.5091\cdot\lambda_{//}+0.4909\cdot\lambda_{\perp}=0.6901\cdot\lambda_{\text{ME, upper}}+0.3099\cdot\lambda_{\text{ME, lower}} & \text{(Kelvin)},\\ 0.4942\cdot\lambda_{//}+0.5058\cdot\lambda_{\perp}=0.6691\cdot\lambda_{\text{ME, upper}}+0.3309\cdot\lambda_{\text{ME, lower}} & \text{(Weaire-Phelan)}.\end{cases} \tag{10}$$

5 Conclusions

The effective thermal conductivity and thermal tortuosity of porous media with different morphologies across a wide range of porosity were analyzed. The conclusions could be drawn as follows.

(1) The equivalent thermal conductivity of the porous skeleton increases with the increase in its volume fraction. Under the same strut porosity, the equivalent thermal conductivity of Kelvin and Weaire-Phelan structures is similar, which is larger than that of the real foam structure. The thermal tortuosity of real foam structure is relatively larger and the heat conduction path becomes straighter by adopting the anisotropic design with elliptical shapes.

(2) The equivalent thermal conductivity and thermal tortuosity of the fluid channels are comparable among different porous structures. Because of the high porosity, the thermal tortuosity of the fluid channels for the Kelvin, Weaire-Phelan, and real foam structures is close to one.

(3) The thermal conductivity of porous structures with a heat transfer fluid increases with an increasing thermal conductivity ratio of fluid and solid. A small porosity of porous media leads to larger equivalent thermal conductivity due to the dominant contribution of porous skeleton in the heat conduction process. Correlations derived from parallel and series models as well as the Maxwell-Eucken models provide decent predictions of the effective thermal conductivity, with an average error lower than 8% across the entire range of thermal conductivity ratios.

This work was supported by the National Natural Science Foundation of China (Grant Nos. 52306272 and 52341601).

1 Mujeebu M A, Abdullah M Z, Bakar M Z A, et al. Applications of porous media combustion technology – A review. Appl Energy, 2009, 86: 1365–1375
2 Rashidi S, Kashefi M H, Kim K C, et al. Potentials of porous materials for energy management in heat exchangers – A comprehensive review. Appl Energy, 2019, 243: 206–232
3 He Y L, Du S, Shen S. Advances in porous volumetric solar receivers and enhancement of volumetric absorption. Energy Rev, 2023, 2: 100035
4 Zhang S, Feng D, Shi L, et al. A review of phase change heat transfer in shape-stabilized phase change materials (ss-PCMs) based on porous supports for thermal energy storage. Renew Sustain Energy Rev, 2021, 135: 110127
5 Zhao C B, Hobbs B, Ord A. Near-field performance of chemical dissolution-front instability around a circular acid-injection-well in fluid-saturated porous media. Sci China Tech Sci, 2023, 66: 2025–2035
6 Du S, Li M J, He Y, et al. Experimental and numerical study on the reflectance losses of the porous volumetric solar receiver. Sol Energy Mater Sol Cells, 2020, 214: 110558
7 Du S, Li Z Y, He Y L, et al. Experimental and numerical analysis of the hydraulic and thermal performances of the gradually-varied porous volumetric solar receiver. Sci China Tech Sci, 2020, 63: 1224–1234
8 Petrasch J, Schrader B, Wyss P, et al. Tomography-based determination of the effective thermal conductivity of fluid-saturated reticulate porous ceramics. J Heat Transfer, 2008, 130: 032602
9 Zafari M, Panjepour M, Davazdah Emami M, et al. Microtomography-based numerical simulation of fluid flow and heat transfer in open cell metal foams. Appl Thermal Eng, 2015, 80: 347–354
10 Ranut P, Nobile E, Mancini L. High resolution microtomography-based CFD simulation of flow and heat transfer in aluminum metal foams. Appl Thermal Eng, 2014, 69: 230–240
11 Bodla K K, Murthy J Y, Garimella S V. Microtomography-based simulation of transport through open-cell metal foams. Numer Heat Transfer Part A-Appl, 2010, 58: 527–544
12 Ranut P, Nobile E, Mancini L. High resolution X-ray microtomography-based CFD simulation for the characterization of flow permeability and effective thermal conductivity of aluminum metal foams. Exp Thermal Fluid Sci, 2015, 67: 30–36
13 Mendes M A A, Ray S, Trimis D. A simple and efficient method for the evaluation of effective thermal conductivity of open-cell foam-like structures. Int J Heat Mass Transfer, 2013, 66: 412–422
14 Bianchi E, Schwieger W, Freund H. Assessment of periodic open cellular structures for enhanced heat conduction in catalytic fixed-bed reactors. Adv Eng Mater, 2016, 18: 608–614
15 Bracconi M, Ambrosetti M, Maestri M, et al. A fundamental analysis of the influence of the geometrical properties on the effective thermal conductivity of open-cell foams. Chem Eng Process, 2018, 129: 181–189
16 Fiedler T, Solórzano E, Garcia-Moreno F, et al. Lattice monte Carlo and experimental analyses of the thermal conductivity of random-shaped cellular aluminum. Adv Eng Mater, 2009, 11: 843–847
17 Wang N, Kaur I, Singh P, et al. Prediction of effective thermal conductivity of porous lattice structures and validation with additively manufactured metal foams. Appl Thermal Eng, 2021, 187: 116558
18 Fu J, Thomas H R, Li C. Tortuosity of porous media: Image analysis and physical simulation. Earth-Sci Rev, 2021, 212: 103439
19 Haussener S, Coray P, Lipiński W, et al. Tomography-based heat and mass transfer characterization of reticulate porous ceramics for high-temperature processing. J Heat Transfer, 2009, 132: 023305
20 Kumar P, Topin F, Vicente J. Determination of effective thermal conductivity from geometrical properties: Application to open cell foams. Int J Thermal Sci, 2014, 81: 13–28
21 Xu W, Jia M, Gong Z. Thermal conductivity and tortuosity of porous composites considering percolation of porous network: From spherical to polyhedral pores. Compos Sci Tech, 2018, 167: 134–140
22 Zhao Z, Zhou X P, Qian Q H. Fracture characterization and permeability prediction by pore scale variables extracted from X-ray CT images of porous geomaterials. Sci China Tech Sci, 2020, 63: 755–767
23 Du S, Li M J, Ren Q, et al. Pore-scale numerical simulation of fully coupled heat transfer process in porous volumetric solar receiver. Energy, 2017, 140: 1267–1275
24 Du S, Tong Z X, Zhang H H, et al. Tomography-based determination of Nusselt number correlation for the porous volumetric solar receiver with different geometrical parameters. Renew Energy, 2019, 135:

711–718
25 Dietrich B, Schell G, Bucharsky E C, et al. Determination of the thermal properties of ceramic sponges. Int J Heat Mass Transfer, 2010, 53: 198–205
26 Meinicke S, Dietrich B, Wetzel T. Pore-scale numerical analysis of hydrodynamics and conjugate heat transfer in solid sponges. In: International Heat Transfer Conference 16. Beijing, 2018
27 Rezaei E, Barbato M, Gianella S, et al. Pressure drop and convective heat transfer in different SiSiC structures fabricated by indirect additive manufacturing. J Heat Transfer, 2020, 142: 032702
28 Rieks S, Wende M, Preußer N, et al. A hydrodynamic analogy based modelling approach for zero-gravity distillation with metal foams. Chem Eng Res Des, 2019, 147: 615–623
29 Ranut P. On the effective thermal conductivity of aluminum metal foams: Review and improvement of the available empirical and analytical models. Appl Thermal Eng, 2016, 101: 496–524